OPTIMIZATION OF MANDOOR AND VENTILATION OPENINGS OF TUBULAR STEEL WIND TURBINE TOWERS WITH RESPECT TO BUCKLING

Charis J. Gantes[1*], Stelios Vernardos[1], Konstantina G. Koulatsou[1], Aysel E. Doğanlı[2], Onur Güneş[2]

[1]School of Civil Engineering, Institute of Steel Structures, National Technical University of Athens
[2]Ateş Wind Power, Izmir, Turkey
[*]chgantes@central.ntua.gr

ABSTRACT
As wind turbine towers grow in height and their blades become longer, actions on the towers are also increased, hence their weight as well, and their safe and cost-effective design becomes critical for the further development of the wind energy sector. One potential failure mechanism of tubular steel towers is shell local buckling. The areas near man door and ventilation openings are locally weakened and are therefore primarily prone to local buckling. In the present paper, the buckling behavior of a tubular steel wind turbine tower is investigated numerically, focusing on the buckling response near such openings. To that effect, nonlinear finite element analyses accounting for geometrical and material nonlinearity and imperfections (GMNIA) is employed. GMNIA is performed taking into account initial geometric imperfections with the shapes resulting from the relevant buckling modes. Different wind directions are considered. Moreover, to investigate the influence of the stiffening of the manhole to the tower buckling strength, a comparison between different alternatives of stiffened and unstiffened openings is performed.

1. INTRODUCTION

As wind energy is gaining great attention as a mature type of cost-effective renewable energy, investigation on wind turbines becomes continuously more interesting. In order to better exploit the available wind potential, wind turbine towers grow in height and their blades become longer. As a result, actions on the towers are also increased and their safe and cost-effective design is important for the further development of the wind energy sector.

In recent years, the most common type of a wind turbine tower is the free-standing tubular steel tower, which is composed of a number of cylindrical and/or conical shells. Its construction is achieved by (i) cold-curving flat steel plates into the desired cylindrical or conical shape, (ii) welding the two edges, to obtain a closed shell, usually 2.5 m to 3.0 m long, as imposed by the industrially available steel plates, (iii) welding consecutive shell parts together, to obtain 20 m to 30 m long shells, as imposed by transportability constraints, (iv) transporting these parts to the wind park site by trucks, lifting them by means of cranes or helicopters and bolting them together with fully preloaded bolts, using pre-welded double ring flanges.

The bottom part of the tower comprises a manhole opening, to accommodate access to the interior of the tower and to the staircase and elevator to the tower top, for maintenance of the electrical and mechanical parts (Figure 1). In many cases, ventilation openings are also foreseen at different height (Figure 2). Such openings weaken the tower shell, inducing stiffness reduction, stress concentrations and increased danger of local buckling. Different measures, such as increase of thickness and placement of a peripheral frame and/or stiffeners are used to counter the negative effects of the manhole.

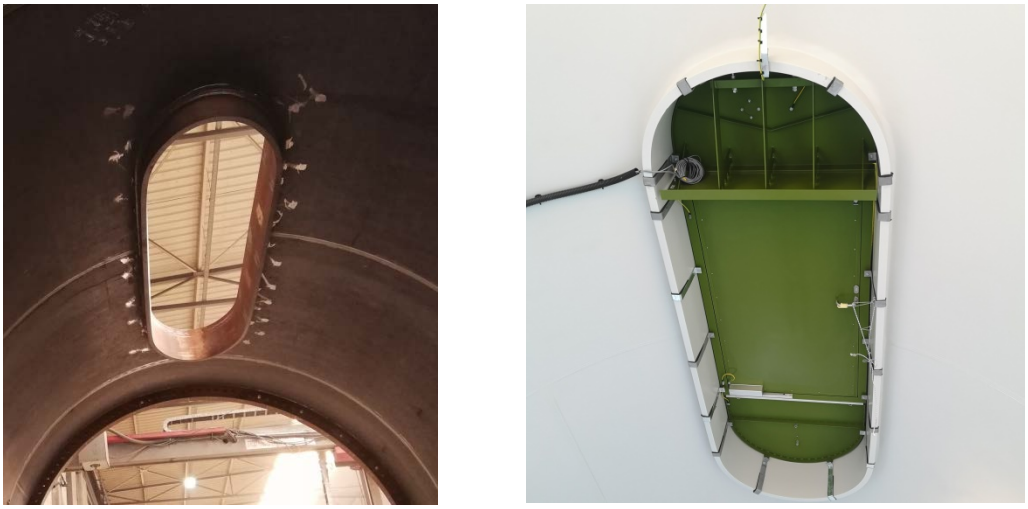

(a) (b)

Figure 1. Photos of typical man-door openings **(a)** during fabrication **(b)** in the finished state

(a) (b)

Figure 2. Photos of typical ventilation openings **(a)** during fabrication **(b)** in the finished state

The effect of an unstiffened or stiffened cutout on the strength of cylindrical steel shells with geometry and slenderness corresponding to modern wind turbine towers under static loads causing bending, has been studied experimentally as well as numerically in [1-3] and under dynamic loads in [4] and in [5-8].

In general, wind loads are the cause of the two most common types of structural failures, either buckling failure of the tower itself, or fatigue failure at its connections. Tower design issues are addressed in [8-20]. Moreover, resonance issues can be also critical for wind turbine towers of significant height and mass at the top [21], [22].

The objective of the present research is to investigate the buckling behavior of a tubular wind turbine tower under realistic wind loads, and more specifically, the buckling response near the man door and ventilation openings. To that effect, nonlinear finite element analyses accounting for geometrical and material nonlinearity and imperfections (GMNIA) is employed. This complements previous buckling investigations by means of analytical verification according to EN1993-1-6 and numerical verification via non-linear finite element analysis [23-25].

2. MAN-DOOR OPENINGS

2.1 Geometry

For the purpose of the present investigation, a wind turbine is considered having a tower of approximately 120 m height. The tower consists of six cylindrical parts and one conical part at the top, which are transported from the factory to the site and are erected and bolted together on site with preloaded bolts. The lower six parts have a constant outer diameter equal to D_{ext}=4300 mm, while their thickness varies along the height of the tower from t=60 mm at the base to t=17 mm at the top. The manhole of the tower is located near the base and has the geometry illustrated in Figure 3.

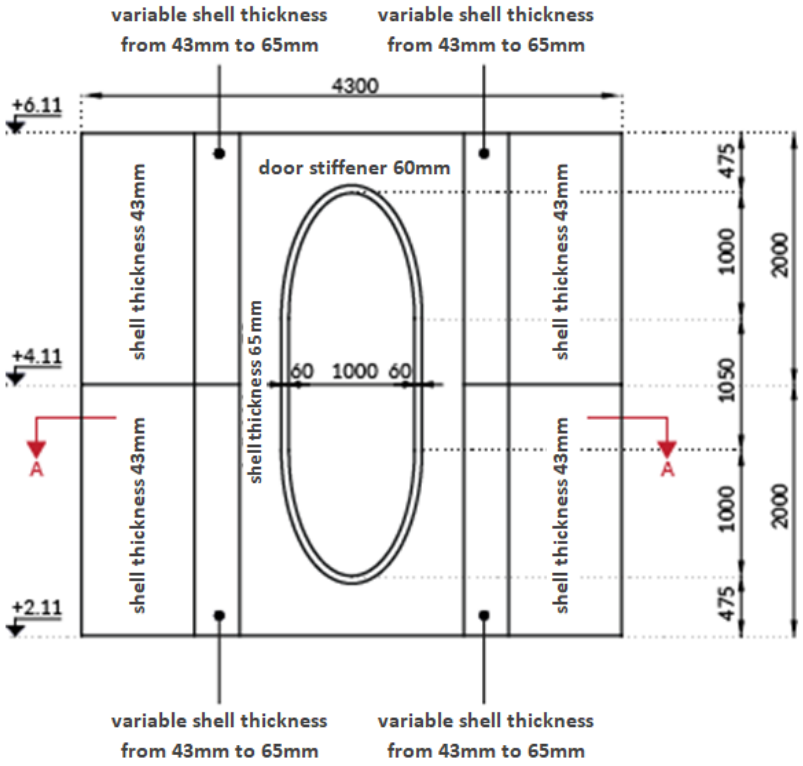

(a) Front view of manhole (dimensions in mm)

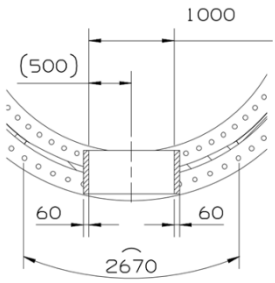

(b) Horizontal section of manhole (section A-A, dimensions in mm)

Figure 3. Geometry of manhole of wind turbine tower under investigation

2.2 Numerical Model

While it would have been ideal to model all parts of the tower with 3d solid finite elements, a lighter and easier to handle numerical model is adopted, using shell finite elements, as described below. An investigation regarding the different types and meshing of finite elements has also been addressed in [23].

As described above, buckling investigation is restricted at the man-door area of the wind turbine tower and in order to assess the buckling potential in this area, the numerical model consists of the tower shell from the bottom of the wind turbine up to the first ring flange connection above the manhole.

The tower shell is modelled with shell elements while the ring flanges with beam elements representing the section of both flanges assumed to act together, taking into account the geometrical eccentricity between flange axis and shell mid-surface by means of rigid elements. It is noted that the parts with variable shell thickness illustrated in Figure 3 are conservatively modeled with the smallest thickness.

The lower shell part is fixed at its base, while the upper part is free at its top, where the second ring flange connection is located. All shell nodes at the top of the model are bound to a rigid constraint with a master node at the geometric center of the tower, where loads are applied.

2.3 Imposed Loads

In order to investigate the tower's buckling behavior, realistic action effects in normal and extreme conditions are taken into account. The design forces and moments are presented in Table 1, which are imposed on the numerical model at the upper flange, at the center master node of the rigid constraints described in section 2.2. Torsional moments are excluded for simplicity.

Table 1. Design loads

	F_y (kN)	F_z (kN)	M_x (kNm)
Z, Y, X	-1225	-7840	135950

2.4 Analysis Method

Initially, linearized buckling analyses (LBA) are performed, using the general-purpose finite element software ADINA v.9.6. It is pointed out that critical buckling loads obtained from LBA are not representative of strength, as material yielding, and effect of imperfections is not taken into account. The purpose of carrying out such analyses is to obtain buckling modes, which are then used as shapes of initial imperfections for the subsequent nonlinear analyses [25].

Next, nonlinear finite analysis considering geometrical and material nonlinearity and initial imperfections (GMNIA) are performed. The ultimate loads obtained from GMNIA are representative of strength and are an appropriate measure of comparison of the considered alternative cases [25].

The finite-element model comprised a total number of approximately 19000 shell elements of varying size, ranging from 40 to 90 mm. The mesh was derived following a sensitivity analysis, which was finalized as soon as further mesh refinement produced no essential differences in terms of both ultimate load and overall behavior. The loads were applied in a quasi-static fashion and the arc-length method was used to obtain the non-linear equilibrium path of the model, pre- and post-collapse. The analyses were run on an Intel Xeon 2.20 GHz CPU with 64 GB of RAM and the required time for each nonlinear analysis was between 5 and 10 minutes.

2.5 Considered Cases

For reasons of comparison, six (6) alternative configurations have been analyzed:

- Case 1: no hole (theoretical case if there was no need for a man-door)
- Case 2: hole - no thickening - no stiffeners (same as the basic design of Figure 3, but without stiffener frame and without thickening)
- Case 3: hole – thickening - stiffeners (same as the basic design of Figure 3)
- Case 4: hole – no thickening - stiffeners (same as the basic design of Figure 3, but without thickening, only with stiffener frame)
- Case 5: hole –thickening - no stiffeners (same as the basic design of Figure 3, but without stiffener frame, only with thickening)
- Case 6: hole –thickening 75 mm - no stiffeners (same as the basic design of Figure 3, but without stiffener frame, only with thickening equal to 75 mm instead of 65 mm)

2.5 Analysis results

The deformed configuration at failure for the considered alternative cases, as obtained from GMNIA, are illustrated in Figure 4. It is interesting to observe how the existence of a man-door opening and the strengthening type control the location and type of local buckling.

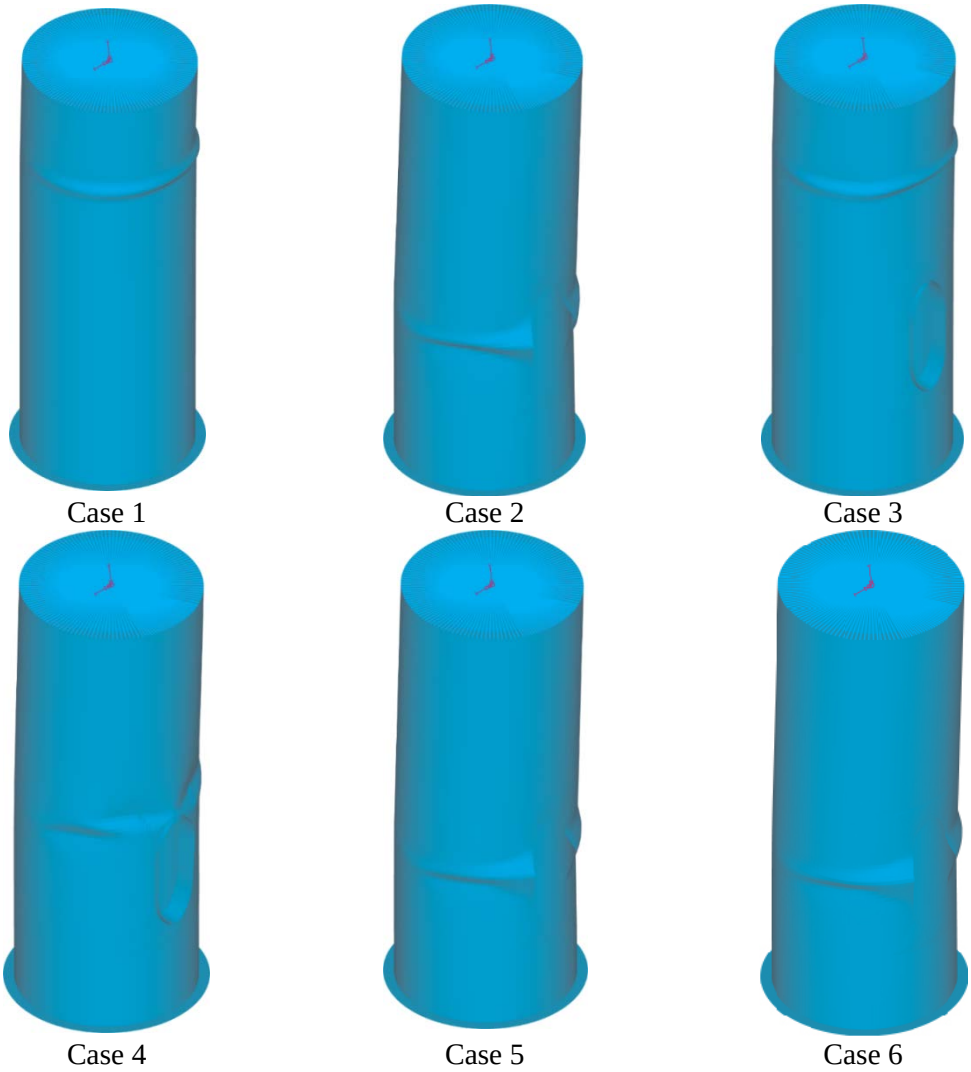

Figure 4. Deformed configuration at failure for the considered alternative cases from GMNIA

Moreover, the von Mises stress distributions at failure for the considered cases 3, 4 and 5, as obtained from GMNIA, are illustrated in Figure 5. Stress concentrations, denoted with red color, are encountered at the same locations where the wrinkles occur in the deformed shapes of Figure 4.

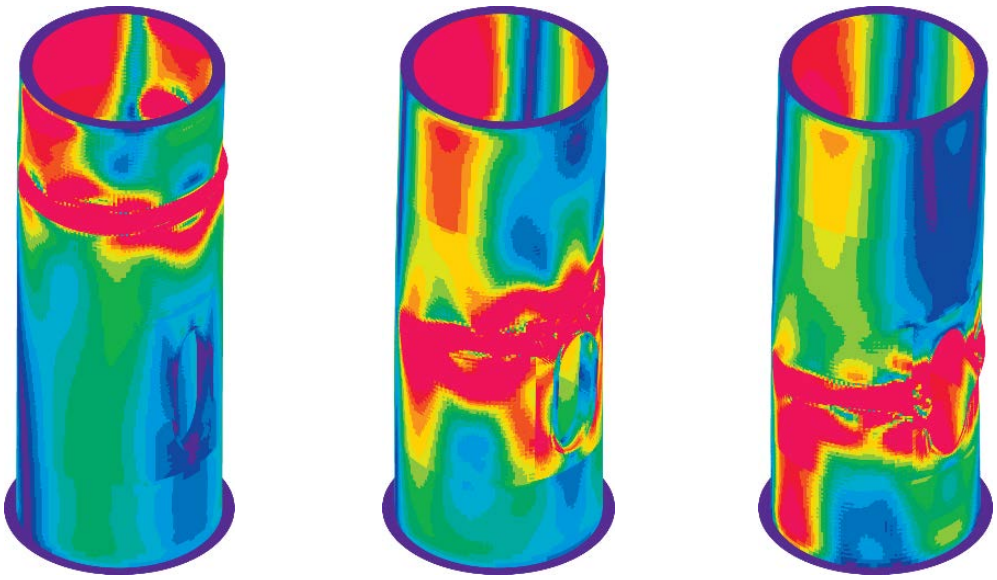

Case 3 Case 4 Case 5

Figure 5. Stress distributions at failure for some of the considered alternative cases from GMNIA

Finally, equilibrium paths obtained from GMNIA for all considered cases are presented in Figure 6. In the vertical axis a load multiplier of the design loads listed in Table 1 is plotted, while the horizontal axis contains the lateral displacement of the top of the modelled part of the tower.

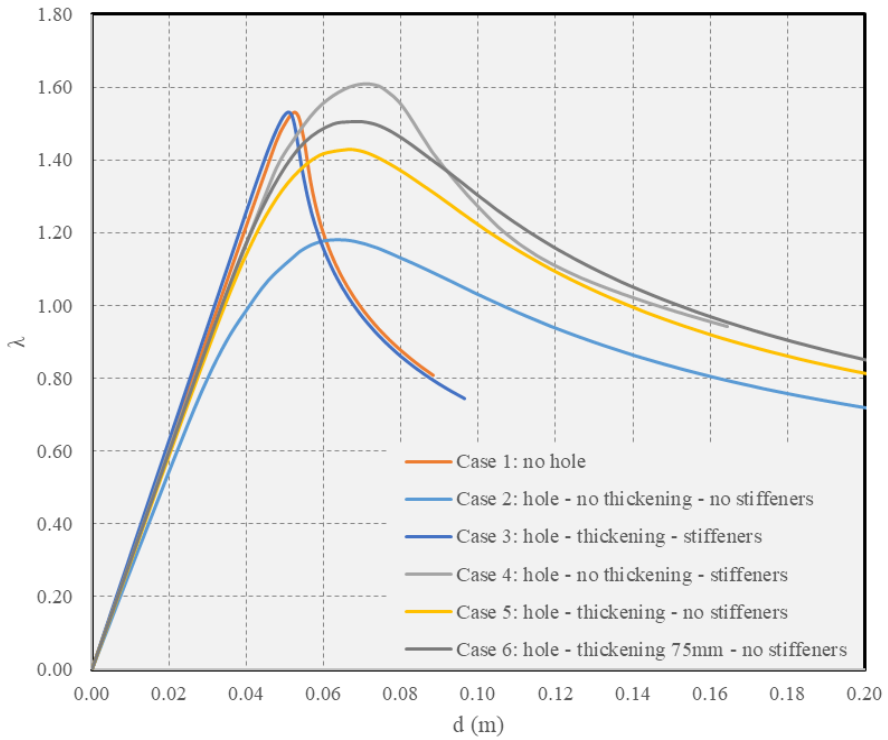

Figure 6. Equilibrium paths for the considered alternative cases from GMNIA

2.6 Discussion

From the equilibrium paths of Figure 6 it is first noted that all curves reach higher loads than the considered design loads (λ=1). Hence, from buckling point of view all designs can be considered as acceptable. The basic design (Case 3) compensates fully for the loss of stiffness and strength due to the manhole, as its equilibrium path is almost the same to the one of Case 1 with no hole. It is further noted in the deformed shapes of Figure 4 that in cases 1 and 3 the buckle occurs at the same place, while in the other four cases the buckle has moved downwards.

The equilibrium path of Case 2, without stiffener frame and without thickening, is much lower, is not recommended and is only shown here for comparison purposes. It is noted also that in this case loss of stiffness starts at much lower load levels, which is also undesirable from the point of view of resonance. All other curves retain almost the same stiffness up to λ=1, meaning that vibration frequencies would be almost same for all of them, hence these solutions are equivalent from resonance check point of view.

The alternative design of Case 4, with stiffener frame but without thickening, has same initial stiffness as the basic design, starts losing stiffness at lower loads, has actually a little higher strength, and has a smoother degradation after the limit point, which is beneficial as it implies higher ductility. Overall, it seems to respond adequately, even a little better than basic design.

The alternative design of Case 5, with thickening but without stiffener frame, has same initial stiffness, starts losing stiffness at even lower loads, has lower strength, and has also a smoother degradation after the limit point, thus higher ductility. Overall, it does not seem to respond adequately.

However, if the door plate thickness increases further, from 65 mm to 75 mm (Case 6), the curve is shifted upwards and leads to practically same strength as the basic design. Eliminating the stiffener frame is desirable from fabrication point of view, considering the need for separate procurement of stiffener frames and the necessary welding effort.

Finally, it is noted that fatigue has not been considered in this investigation. The different solutions have been compared only from buckling point of view, and indirectly from resonance point of view. It is, however, expected, that elimination of welded stiffener frame will be also beneficial in terms of fatigue verification.

3. VENTILATION OPENINGS

3.1 Geometry

A similar investigation as for man-door openings has been conducted for ventilation openings, considering the geometry illustrated in Figure 7. In this example, two ventilation openings are arranged at the two ends of a section diameter, near the tower base. Numerical modeling and analysis have been conducted in the same way as described for man-door openings in section 2.

3.2 Loading

For simplicity, same loads as for the man-door openings have been used. Exact loading values are not important regarding the comparative evaluation of different designs with/without stiffener frames; however, it is important for the direct assessment of safety factors. Keeping the magnitude of the aforementioned loads constant, three different angles within a quarter-circle (due to the symmetry of this tower section) were examined in search of the worst-case scenario, as shown in Figure 8.

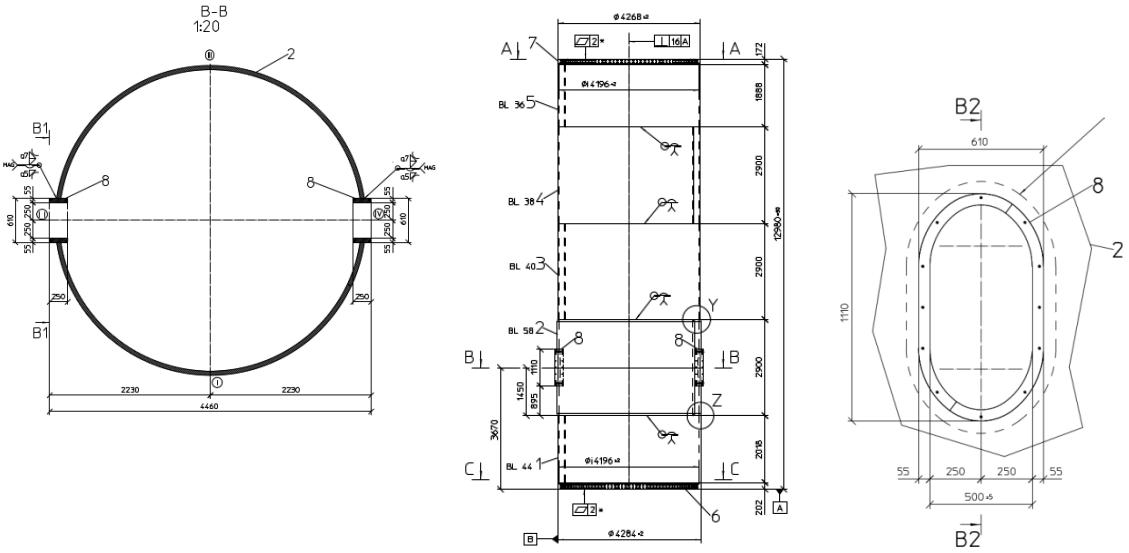

Figure 7. Geometry of ventilation opening under investigation

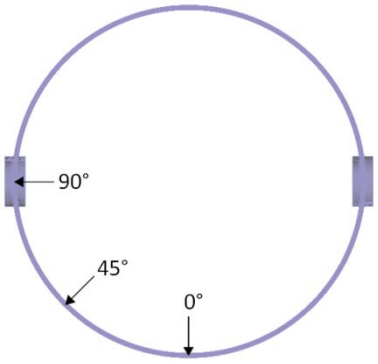

Figure 8. Considered wind directions

3.3 Effect of Wind Direction

As demonstrated by the load-displacement curves of Figure 9, the 90° angle leads to a slightly lower ultimate load. It is also noticeable that both the 45° and 90° angles result in a less ductile behavior. The 90° angle is thus used for further investigations.

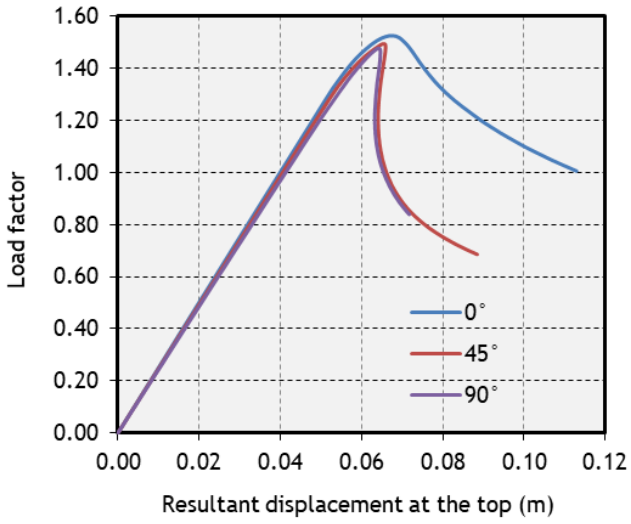

Figure 9. Comparison of equilibrium paths for the considered wind directions

3.4 Effect of Stiffener Framing

A comparison between the tower section's response with and without frames around the ventilation openings is first presented, in terms of deformation shapes and magnitudes, von Mises stress distributions and load-displacement curves (Figures 10 and 11). Failure occurs due to local buckling at the uppermost part of the tower section. Yielding is observable at the level of buckles on both the compressed and tensed side. No essential enhancement due to the frames' presence is observable.

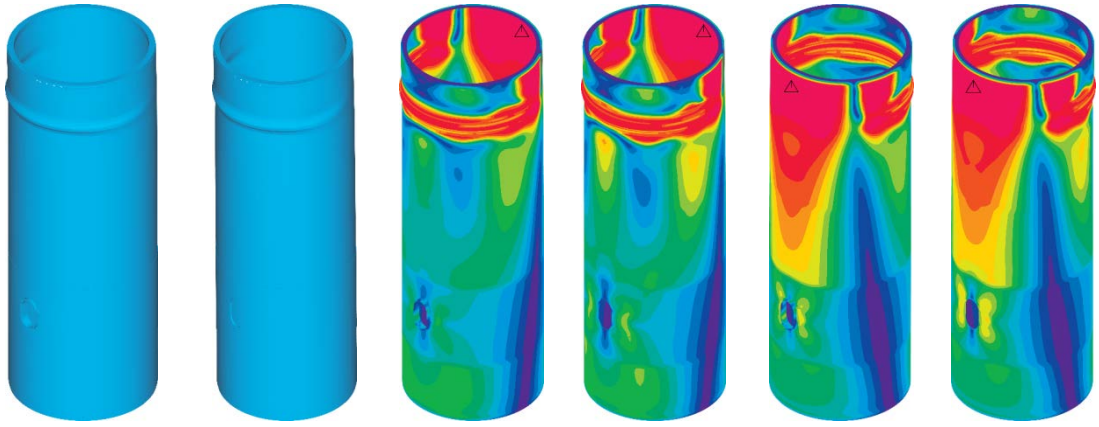

Deformed shape with (left) and without (right) frames

Von-Mises stress distribution at the compressed side with (left) and without (right) frames

Von-Mises stress distribution at the tensed side with (left) and without (right) frames

Figure 10. Comparison of deformation and stress distribution at failure with and without stiffener frames

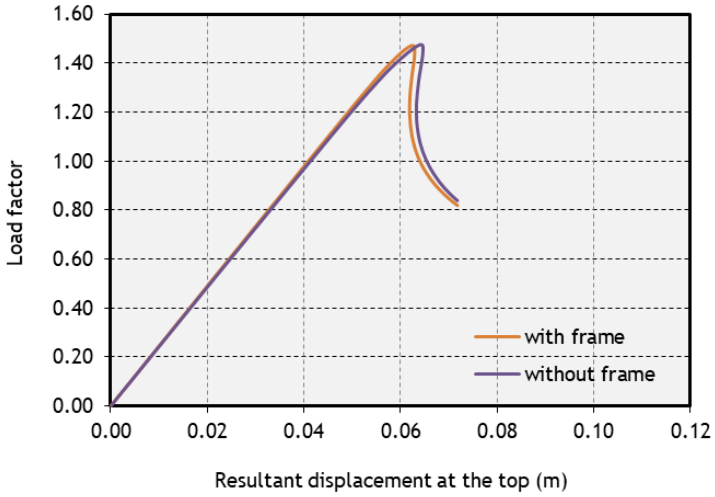

Figure 11. Comparison of equilibrium paths with and without stiffener frames

3.5 Effect of Door Plate Thickness

Omitting the frames from both ventilation openings, the shell thickness of the part bearing the ventilation openings is investigated. The results of three analyses are indicatively shown in Figures 12 and 13, pertaining to a shell thickness of 44 mm (same as the shell thickness of the lower part), 48 mm and 58 mm. It can be observed that lowering of the shell thickness results in a more ductile behavior and a decreased ultimate load and stiffness. However, it appears that with a thickness of 48 mm, the benefits of less material and increased ductility come with a small sacrifice in ultimate load and stiffness.

Deformed shape without frames with shell thickness of (left to right) 44 mm, 48 mm and 58 mm

Von Mises stress distribution of the compressed side without frames with shell thickness of (left to right) 44 mm, 48 mm and 58 mm

Figure 12. Comparison of deformation and stress distribution at failure without stiffener frames for varying door plate thickness

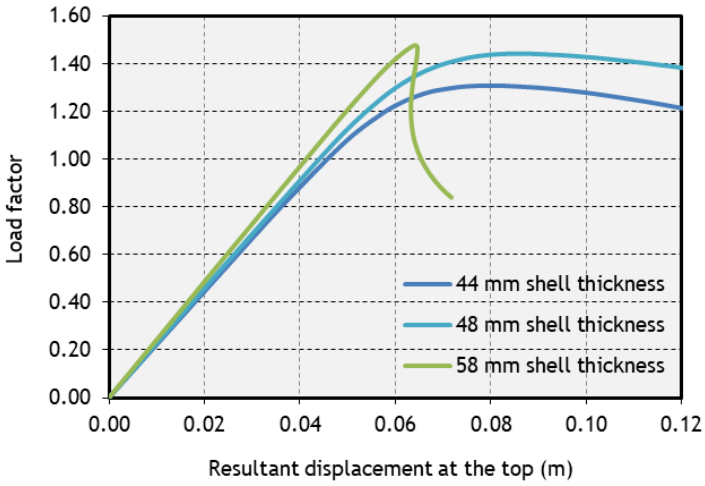

Figure 13. Comparison of equilibrium paths without stiffener frames for varying door plate thickness

4. SUMMARY AND CONCLUSIONS

The buckling response of tubular steel wind turbine towers in the presence of openings has been investigated by means of fully nonlinear finite element analyses. Large openings used as man-doors as well as smaller openings used for ventilation have been addressed. The presence of the openings causes stress concentrations and increased local buckling danger. Alternative strengthening schemes have been compared, employing a peripheral stiffener frame, a thicker door plate or a combination of the two. The results indicate a reasonably thicker door plate is sufficient to recover the lost stiffness and strength due to the opening, and that the costlier and cumbersome from fabrication point of view stiffener frame can be eliminated. Pending experimental validation and fatigue verification, this may be an interesting direction towards reducing the time and cost of wind turbine tower fabrication.

REFERENCES

[1] **Dimopoulos, C.A., Gantes, C.J.,** (2012) *Experimental Investigation of Buckling of Wind Turbine Tower Cylindrical Shells with Opening and Stiffening under Bending.* Thin-Walled Structures, 54, p. 140-155.

[2] **Dimopoulos, C.A., Gantes, C.J.,** (2013) *Comparison of Stiffening Types of the Cutout in Tubular Wind Turbine Towers*. Journal of Constructional Steel Research, 83, p. 62–74.

[3] **Dimopoulos, C.A., Gantes, C.J.,** (2015) *Numerical Methods for the Design of Cylindrical Steel Shells with Unreinforced or Reinforced Cutouts*. Thin-Walled Structures, 96, p. 11-28.

[4] **Dimopoulos, C.A., Koulatsou, K.G., Petrini, F., Gantes, C.J.,** (2015) *Assessment of Stiffening Type of the Cutout in Tubular Wind Turbine Towers under Artificial Dynamic Wind Actions*. Journal of Computational and Nonlinear Dynamics (ASME), 10(4), 041004-1 - 041004-9.

[5] **Brogan, F., Almorth, B.O.,** (1970) *Buckling cylinders with cutout.* AIAA, 8 (2), p. 236-240.

[6] **Almorth, B.O., Holmes, A.M.C.,** (1972) *Buckling of shells with cutouts, experiment and analysis.* International Journal of Solids and Structures, 8, p. 1057-1071.

[7] **Bennet, R., Dove, R.C., Butler, T.A.,** (1981) *An investigation of buckling of steel cylinders with circular cutouts reinforced in accordance with ASME RULES.* Rep. Los Alamos Scientific Laboratory, NUREG/CR-2165 LA-8853-MS.

[8] **Salmi, P., Ala-Outinen, T.,** (1997) *Cylindrical shell structures from austenitic stainless under meridional compression*. Rep. VTT 1897 – Technical Research Centre of Finland.

[9] **Calladine, C.R.,** (1980) *Theory of Shell Structures*. Cambridge University Press.

[10] **Teng, J.G., Rotter, J.M.,** (2004) *Buckling of Thin Metal Shells*. Spon Press, London.

[11] **Bazeos, N., Hatzigeorgiou, G.D., Hondros, I.D., Karamaneas, H., Karabalis, D. L., Beskos, D. E.,** (2002) *Static, Seismic and Stability Analyses of a Prototype Wind Turbine Steel Tower*. Engineering Structures, 24, p. 1015-1025.

[12] **Lavassas, I., Nikolaidis, G., Zervas, P., Efthimiou, E., Doudoumis, I.N., Baniotopoulos, C. C.,** (2013) *Analysis and Design of the Prototype of a Steel 1-MW wind turbine tower.* Engineering Strucutres, 25, p. 1097-1106.

[13] **Zhao, Z., Dai, K., Camara, A., Bitsuamlak, G., Sheng, C.,** (2019) *Wind Turbine Tower Failure Modes under Seismic and Wind Loads.* Journal of Performance of Constructed Facilities, 33 (2).

[14] **Petersen, C.,** (1993) *Stahlbau: Grundlagen der Berechnung und baulichen Ausbildung von Stahlbauten.* Vieweg.

[15] **Petersen, Ch.,** (1998) *Nachweis der Betriebsfestigkeit exzentrisch beanspruchter Rinf-flanschverbindungen*, Stahlbau, 67, Heft 3.

[16] **Wang, Y.Q., Zong, L., Shi, Y.J.,** (2013) *Bending Behavior and Design Model of Bolted Flange-Plate Connection*, Journal of Construction Steel Research, 84, p. 1-16.

[17] **Hoang, V.L., Jaspart, J.P., Demonceau, J.F.,** (2013) *Behavior of Bolted Flange Joints in Tubular Structures under Monotonic, Repeated and fatigue Loadings I: Experimental Tests*, Journal of Construction Steel Research, 85, p. 1-11.

[18] **Nussbaumer, A., Borges, L., Davaine, L.,** (2018) *Fatigue Design of Steel and Composite Structures*, 2nd edition, ECCS-European Convention for Structural Steelwork.

[19] **Mikitarenko, M.A., Perelmuter, A.V.,** (1998) *Safe fatigue life of steel towers under the action of wind vibrations*, Journal of Wind Engineering and Industrial Aerodynamics, p. 74-76, 1091-1100.

[20] **Nuta, E., Christopoulos, C., Packer, J.A.,** (2011) Methodology for seismic risk assessment for tubular steel wind turbine towers: application to Canadian seismic environment. Canadian Journal of Civil Engineering, 38, p. 293–304.

[21] **Takewaki, I.,** (1996) *Optimal Frequency Design of Tower Structures via an Approximation Concept*. Computers and Structures, 58 (3), p. 445-452.

[22] **Takewaki, I.,** (1997) *Efficient Optimal Frequency Design of Elastically Supported Distributed-Parameter Cantilevers*. Computers and Structures, 62 (1), p. 107-117.

[23] **Koulatsou, K.G., Chondrogiannis, K.-A., Gantes, C.J.,** (2019) *Structural Optimization of Tubular Steel Wind Turbine Towers with Respect to Buckling.* Proceedings of the IASS Annual Symposium 2019 – Structural Membranes 2019, *Form and Force*. Spain, p. 823-830.

[24] **European Committee for Standardization.,** (2007), *Eurocode 3: Design of Steel Structures – Part 1.6: Strength and Stability of Shell Structures*.

[25] **Gantes, C.J., Fragkopoulos, K.A.,** (2010) *Strategy for Numerical Verification of Steel Structures at the Ultimate Limit State*, Structure & Infrastructure Engineering, 6, p. 225–255.